

1

2 **Revalorization of cellulosic wastes from *Posidonia oceanica* and *Arundo donax* as catalytic**
3 **materials based on affinity immobilization of an engineered β -galactosidase**

4

5

6

7 María José Fabra¹, Isabel Seba-Piera¹, David Talens-Perales¹, Amparo López-Rubio¹,
8 Julio Polaina¹, Julia Marín-Navarro^{1,2} *

9

10

11 ¹*Instituto de Agroquímica y Tecnología de Alimentos, CSIC, Valencia, Spain*

12 ²*Departamento de Bioquímica y Biología Molecular, Universidad de Valencia, Spain.*

13

14

15 *Corresponding author.

16 *E-mail address: juvicma@uv.es*

17

18 **Abstract**

19 Catalytic materials obtained by enzyme immobilization have multiple potential
20 applications in the food industry. The choice of the immobilization method and support
21 may be critical to define the properties of the immobilized enzyme compared to the
22 soluble form. Although the use of immobilized enzymes shows multiple advantages,
23 their catalytic efficiency is compromised in many instances. Molecular engineering
24 techniques have been used to generate hybrid proteins where the enzyme of interest is
25 fused to a module with affinity to a specific biopolymer. Binding of the hybrid TmLac-
26 CBM2 protein, in which the β -galactosidase from *Thermotoga maritima* is fused to a
27 carbohydrate-binding module from *Pyrococcus furiosus*, to cellulosic material from
28 aquatic biomass wastes (such as *Posidonia oceanica* and *Arundo donax*) has been
29 assayed. Both species generate environmental wastes that could be revalorized if
30 converted into bioactive materials. Cellulose cryogels, but not films, from *P. oceanica*
31 were able to bind the TmLac-CBM2 hybrid, with a higher immobilization yield (90 %)
32 than that from *A. donax* cellulose cryogels (60 %). However, fractions containing also
33 hemicellulose were less effective as immobilization supports in both cases, with yields
34 of 47 % and 30 %, respectively. Cellulose cryogels loaded with β -galactosidase were
35 able to hydrolyse lactose with the same efficiency as the free form of the enzyme. In
36 contrast, enzyme-loaded cellulose films were inactive. This study represents a proof of
37 concept for the valorisation of cellulosic wastes as bioactive materials. Furthermore, it
38 provides information about the interaction specificity between the binding module and
39 the cellulosic support, useful for other enzymes.

40 **Keywords**

41 Lactase, cellulose, hemicellulose, enzyme bioadsorption, carbohydrate-binding module,
42 bioaffinity-based immobilization

43 **1. Introduction**

44 The development of catalytic materials through enzyme-immobilization is of great
45 interest for the food industry (Yushkova et al., 2019). Nowadays, immobilized enzymes
46 are preferred over their corresponding free forms due to several technical and economic
47 advantages, including improved stability and recovery of products with greater purity.
48 Moreover, enzyme-activated supports can be implemented in continuous processes,
49 applied as biosensors or used in the production of bioactive packaging (Khan, Wen,
50 Huq, & Ni, 2018; Nguyen, Lee, Lee, Fermin, & Kim, 2019; Sharma & Leblanc, 2017;
51 Sheldon & van Pelt, 2013). Several methods are employed for immobilization, mainly
52 based on the adsorption of the enzyme to the support through chemical interactions
53 (either covalent or non-covalent) (Bilal & Iqbal, 2019; Datta, Christena, & Rajaram,
54 2013; Jesionowski, Zdarta, & Krajewska, 2014; Sirisha, Jain, & Jain, 2016; Yushkova
55 et al., 2019).

56 In the food industry, β -galactosidases (EC 3.2.1.23) are biotechnology relevant enzymes
57 with multiple applications related to the production of lactose-free milk and milk
58 derivatives. These enzymes catalyse the hydrolysis of terminal non-reducing β -D-
59 galactose residues from di-, oligo- and conjugated saccharides, including lactose
60 (Husain, 2010). Therefore, β -galactosidases with lactase activity are currently employed
61 to generate lactose-free milk products (Adam, Rubio-Teixeira, & Polaina, 2004), with an
62 increasing demand due to the high prevalence of lactose intolerance among the world
63 population (Harrington & Mayberry, 2008; Itan, Jones, Ingram, Swallow, & Thomas,
64 2010). Based on their hydrolytic properties, β -galactosidases are also used in large scale
65 industrial processes for the treatment of cheese-whey derived from dairy industries to
66 reduce pollution load and to produce sweeteners (Andler & Goddard, 2018; Husain,
67 2010; Oliveira, Guimarães, & Domingues, 2011). Furthermore, these enzymes also

68 catalyse transglycosylation reactions, which can be used to produce added-value
69 products from lactose, such as health beneficial prebiotics (e. g. lactulose or
70 galactooligosaccharides) (Andler & Goddard, 2018; Gänzle, 2012). However, there are
71 some important factors limiting the utilization of β -galactosidases in food applications,
72 for instance, the difficulties associated with recovering enzymes from the final product.
73 Different immobilization techniques and supports have been applied to β -galactosidases
74 (Marín-Navarro, Talens-Perales, Oude-Vrielink, Cañada, & Polaina, 2014; Ricardi et
75 al., 2018; Sen, Nath, Bhattacharjee, Chowdhury, & Bhattacharya, 2014; Urrutia, Bernal,
76 Wilson, & Illanes, 2018; Wolf, Gasparin, & Paulino, 2018; Yushkova et al., 2019).
77 Enzyme immobilization through covalent cross-linking providing multi-point
78 attachment usually results in improved stability (Sheldon & van Pelt, 2013). However,
79 the catalytic efficiency is compromised in many cases. Physical adsorption through
80 electrostatic interactions (e.g. using activated carbon supports) is a simple method and,
81 in general, it affects enzyme activity to a lesser degree than technologies mediated
82 through covalent crosslinking (Jesionowski et al., 2014). Even in this case, enzyme
83 confinement within the immobilization matrix may affect catalytic activity since the
84 conditions of the internal milieu may differ from the bulk solution. Both the chemical
85 characteristics of the solid support and the restrictions imposed to diffusion of substrates
86 and products contribute to the change in the microenvironment of the immobilized
87 enzyme, compared to the free form (Bolivar & Nidetzky, 2019). A particular case of
88 physical adsorption, referred as bioadsorption or affinity immobilization, is based on the
89 affinity of a protein or protein module to a specific substrate (Estevinho et al., 2018;
90 Mislovičová, Masárová, Vikartovská, Gemeiner, & Michalková, 2004). In this context,
91 molecular engineering techniques can be used to create hybrid proteins by fusion of the
92 enzymes to a module with affinity for a specific biopolymer. Such is the case of

93 carbohydrate-binding modules (CBM), which are found in different glycoside
94 hydrolases and are able to bind specific polysaccharides. They are classified into
95 different families by sequence homology, which is related to their substrate specificity
96 (Boraston, Bolam, Gilbert, & Davies, 2004). In a recent work, Estevinho *et al.* (2018)
97 showed the suitability of hydrated and freeze-dried bacterial cellulose (BC) to
98 immobilize a hybrid enzyme composed by a β -galactosidase from *Thermotoga maritima*
99 (TmLac) and a CBM2 from *Pyrococcus furiosus*, with high specificity compared to the
100 non-engineered enzyme. The CBM2 provided a stable attachment of the hybrid enzyme
101 to the BC support at high temperatures. However, initial enzymatic activity of the
102 immobilized enzyme was lower (around 52 %) than that of the free form, probably
103 because of diffusion constraints within the highly compact matrix of BC. Thus,
104 cellulosic materials with different structures may be explored to circumvent this
105 limitation. Moreover, the production cost of BC is usually quite high whereas multiple
106 cellulose sources from agricultural, food or aquatic wastes are available and represent
107 eco-friendly and low-cost alternative materials (Khiari & Belgacem, 2017; Rao &
108 Rathod, 2018).

109 The marine plant *Posidonia oceanica*, which generates a large amount of coastal waste,
110 and, the invasive plant *Arundo donax* are both recognized as important environmental
111 problems (Khiari & Belgacem, 2017; Lambert, Dudley, & Saltonstall, 2010). These
112 species show a high content of cellulose and hemicelluloses (Khiari & Belgacem,
113 2017), which may be used as immobilization supports. The strategy used in this work
114 takes advantage of the potential of these natural resources in line with the current
115 policies focused in bioeconomy and circular economy (Khiari & Belgacem, 2017;
116 Pilavtepe, Celiktas, Sargin, & Yesil-Celiktas, 2013). This study is focused on
117 investigating the potential of lignocellulosic materials obtained from biomass wastes to

118 generate bioactive supports through the immobilization of the hybrid enzyme TmLac-
119 CBM2. Initially, the binding yield of the hybrid enzyme was tested on cellulosic
120 fractions with different degrees of purity, and prepared in different physical forms (film
121 vs. cryogel). On a second stage, the activity of the immobilized enzyme was analysed
122 and compared to that of the free form. This study can be considered a proof of concept
123 relative to the generation of catalytic materials, while taking into consideration different
124 immobilized enzymes through specific interactions between the CBM2 module and the
125 cellulosic support.

126

127 **2. Materials and methods**

128 **2.1 Preparation of hybrid TmLac-CBM2 β -galactosidases**

129 The hybrid enzyme used in this work (TmLac-CBM2) was constructed by fusing a β -
130 galactosidase from *Thermotoga maritima* (TmLac) (Marín-Navarro et al., 2014) with a
131 carbohydrate binding module (CBM2) from *Pyrococcus furiosus* chitinase (Nakamura
132 et al., 2008). The genetic construct encoding the hybrid protein, as well as the
133 production of both TmLac-CBM2 and the wild type TmLac by *Escherichia coli*, have
134 been described in a previous work (Estevinho et al., 2018). Because both TmLac and
135 TmLac-CBM2 are thermoresistant proteins, purification was carried out by heat shock
136 treatment of crude extracts at 85 °C during 10 min. Endogenous *E. coli* proteins
137 precipitated whereas most of the recombinant protein remained in the soluble fraction.
138 This single step purification procedure was selected because it is much more cost-
139 effective and less time-consuming than chromatographic methods. The soluble fraction
140 was dialyzed against phosphate buffer 50 mM pH 6.5 and concentrated by ultrafiltration
141 using a membrane with a 20 KDa cutoff (Thermo Fisher Scientific). Enzyme
142 concentration was determined as the ratio of β -galactosidase activity (expressed in μ mol

143 galactose · min⁻¹ · ml⁻¹ sample) divided by the intrinsic activity of TmLac-CBM2 (28
144 μmol galactose·min⁻¹·mg enzyme⁻¹), as previously described (Estevinho et al., 2018).

145

146 **2.2 Preparation of cellulosic fractions**

147 *Posidonia oceanica* leaves were collected directly from beaches located in Calpe
148 (Valencian Community, Spain) and the stems of *Arundo donax* (common cane) were
149 obtained from a freshwater environment in Buñol (Comunidad Valenciana, Spain). All
150 the materials were thoroughly washed with water to remove impurities like sand/soil
151 and salts.

152 In order to sequentially eliminate the different components of the cell wall and obtain
153 the different lignocellulosic fractions, a purification procedure previously applied to
154 other plant resources was carried out (Benito-González, López-Rubio, & Martínez-
155 Sanz, 2018; Lu & Hsieh, 2012b, 2012a). Initially, a Soxhlet extraction step was carried
156 out to remove wax, pigments and oils. 40 g of ground wet *Posidonia* leaves or *Arundo*
157 *donax* stem biomass (corresponding to approximately 4 g of dry material) were
158 extracted with 800 mL of toluene/ethanol (2:1 v/v) during 24h. The resulting material
159 was dried at room temperature overnight to obtain the first fraction (referred to as F1).
160 Subsequently, the lignin was eliminated by submitting the previously ground de-waxed
161 material (F1) to a 5 h incubation at 70 ° C with 700 mL of a 1.4% NaClO₂ solution,
162 having the pH adjusted to 3 with acetic acid. After that, the reaction was stopped by
163 quenching with ice, and the excess liquid was decanted. The yellowish solid was
164 collected and repeatedly washed with distilled water by vacuum filtration until the
165 filtrate became approximately neutral, thereby obtaining the second fraction (referred to
166 as F2). The de-lignified material was then treated with 400 mL of 5% KOH solution for

167 24 h at room temperature, followed by 2 h at 90 ° C, in order to remove the
168 hemicelluloses, yielding pure cellulose (referred to as F3).

169

170 **2.3 Formation of hydrated cellulose, films and cryogels**

171 Initially, 0.25 g of material were resuspended in 50 mL of 50 mM phosphate buffer at
172 pH 6.5 and dispersed by mild sonication, followed by ultra-turrax homogenization until
173 obtaining homogeneous, viscous suspensions, which were used to prepare hydrated
174 cellulose, films and cryogels.

175 Hydrated cellulose was collected after centrifugation (1500 g for 15 minutes) of the
176 viscous solutions and removal of the excess of solvent by carefully pipetting the
177 supernatant.

178 Films were obtained by filtering the viscous solution using a vacuum pump (Comecta,
179 S.A.) and PTFE filters with 0.2 µm pore size to remove the phosphate buffer. The solid
180 material remaining in the filter was then dried at room temperature overnight. The
181 formed films were peeled off the filters and stored at 0% relative humidity. For
182 comparative purposes, cellulose films were also prepared after incubating 2.5 g of
183 hydrated cellulose (F3) with 4.2 mL of enzyme (as described in section 2.4,
184 immobilization step). After removal of the unbound enzyme, 50 mM phosphate buffer
185 at pH 6.5 was added (up to 50 mL), and the film was formed by filtration as previously
186 described. These films prepared with enzyme-bound cellulose were referred as Enzy-
187 films.

188 The cryogels were prepared by freeze-drying the previously obtained viscous solutions
189 from each of the lignocellulosic phases.

190

191 **2.3 Enzyme immobilization**

192 The immobilization of the hybrid β -galactosidase (TmLac-CBM2) on the different
193 cellulosic matrices was carried out by incubating 30 mg of the material with 0.5 mL of
194 enzyme (0.5 mg/mL) in phosphate buffer 50 mM pH 6.5 under constant stirring (180
195 rpm) for 4 h at 37 °C. Afterwards, unbound enzyme was directly recovered from the
196 supernatant. The lignocellulosic support was then washed once with 1 mL of assay
197 buffer (50 mM phosphate pH 6.5, 10 mM NaCl, 1 mM MgCl₂) to remove the unbound
198 enzyme and the lactase activity of the immobilized enzyme was determined in the
199 lignocellulosic support. Control samples of enzyme without lignocellulosic supports
200 were incubated in parallel under the same conditions. All the assays were performed in
201 triplicate.

202 Immobilization yield (IY) was calculated according to the following formula:

$$203 \text{ IY} = [(C - \text{UB})/C] \cdot 100$$

204 where C and UB correspond to the β -galactosidase activity of the control and unbound
205 samples, respectively.

206

207 **2.4 Enzyme assays**

208 The quantification of β -galactosidase activity was determined at 75 °C using as
209 substrate a 5 mM solution of *p*-nitrophenyl β -D-Galactopyranoside (PNPGal) in the
210 assay buffer (50 mM phosphate pH 6.5, 10 mM NaCl, 1 mM MgCl₂). Enzymatic
211 activity was quantified spectrophotometrically at 400 nm (NanoDrop ND-1000)
212 corresponding to the maximum absorption of the *p*-nitrophenyl.

213 The lactase activity of the free and immobilized enzyme was tested by incubating the
214 lignocellulosic supports with 5 % (w/v) of lactose solution in assay buffer at 75 °C in a
215 final volume of 20 mL. Control samples containing similar enzyme amounts of soluble
216 enzyme were analysed in parallel. The amount of glucose released was quantified using

217 a glucose assay kit (P7119-10CAP, Sigma- Aldrich, Madrid, Spain) by measuring with
218 a UV/Vis spectrophotometer (BeckMan DU530, GMI, Minnesota, USA) at 450 nm.
219 One unit (IU) is defined as the amount of enzyme releasing 1 μ mol of glucose per
220 minute.

221

222 **2.5 Scanning Electron Microscopy (SEM) analysis.**

223 The microstructural analysis of the cryogels was carried out by means of a Scanning
224 Electron Microscope (Hitachi S-4800). Films were cryo-fracturated after immersion in
225 liquid nitrogen and randomly broken to investigate the cross-section of the samples.
226 Cryo-fracturated films and cryogel samples were mounted on aluminium stubs and
227 fixed on the support using a double-size adhesive tape. Finally, samples were gold-
228 palladium coated and observed using an accelerating voltage of 10 kV and a working
229 distance of 10 mm.

230

231 **2.6 Statistical analysis**

232 The statistical analysis of data was carried out by means of IBM SPSS Statistics
233 software (v.23) (IBM Corp., USA) through the analysis of variance (ANOVA). Tukey's
234 Honestly Significant Difference (HSD) was used at the 95% confidence level for
235 multiple comparison tests

236

237 **3. Results and Discussion**

238

239 **3.1. Effect of the physical state of the cellulosic support on the binding yield of the**
240 **enzyme mediated by the CBM2 module**

241 The binding yield of the hybrid TmLac-CBM2 to pure cellulose (F3) from *P. oceanica*
242 in three different physical states: hydrated cellulose, cryogel or film was compared. As
243 shown in Figure 1, the enzyme was successfully immobilized on pure cellulose both in
244 the format of hydrated cellulose and cryogel, with a somewhat higher yield in the latter
245 case. In contrast, the hybrid enzymes were unable to bind to the cellulosic film. This is
246 likely due to the highly compact structure of the film, compared to the cryogel (see
247 Figure 2). The high density of hydrogen bonds interconnecting cellulose fibres within
248 the film probably hampers the interaction with the CBM2 module. Therefore, the
249 cryogel format was selected for further studies.

250 The binding yield of the cellulose cryogel from *P. oceanica* (7.5 mg enzyme/g of
251 support) obtained after incubation of 30 mg of support with 0.25 mg of enzyme was
252 within the range of the values reported for the freeze-dried bacterial cellulose (3.6 - 9.2
253 mg enzyme/g of support), assayed under similar conditions (incubation of 30 mg of
254 support with 0.15 - 0.35 mg of enzyme) (Estevinho et al., 2018). This result suggests
255 that the available number of binding sites in both supports is comparable. In the
256 previous study, immobilization of the TmLac-CBM2 to bacterial cellulose was stable at
257 high temperature, with negligible enzyme leaching after incubation at 75 °C for 3 hours
258 (Estevinho et al., 2018). This indicates that the CBM2 module shows a strong affinity
259 for cellulose, allowing reusability of immobilized chimeric enzymes as long as the
260 catalytic module remains active. A similar result would be expected for *P. oceanica*
261 cellulose.

262

263 **3.2. Analysis of the binding yields of the TmLac-CBM2 hybrid to different**
264 **cellulosic fractions from *P. oceanica* and *A. donax*.**

265 The suitability of less purified cellulosic fractions from *P. oceanica* and *A. donax* for
266 the development of enzymatically active material was also evaluated. Three different
267 cellulosic fractions from *P. oceanica* and *A. donax* were compared as immobilization
268 supports for the TmLac-CBM2 hybrid. Fraction F1 was obtained after the elimination of
269 lipids, pigments and oils from the original sample. Subsequently, F2 was isolated after
270 removal of lignin and finally, F3 was obtained as pure cellulose after separation from
271 hemicelluloses. Fraction F1 from both sources was discarded because it could not be
272 recovered as a cryogel form after freeze-drying, giving rise to a powder which was not
273 easily handled.

274 Figure 3 shows the affinity of TmLac-CBM2 for F2 and F3 supports obtained from both
275 sources. Immobilization yield mediated by the CBM2 module was more efficient with
276 pure cellulose than with the fraction containing hemicellulose. This is a relevant result
277 since CBMs belonging to family 2 are present in a wide range of cellulolytic enzymes
278 including cellulases, chitinases, xylanases and mananases (Lombard, Golaconda
279 Ramulu, Drula, Coutinho, & Henrissat, 2014). Thus, carbohydrates as cellulose, chitin,
280 xylan and manan are potential substrates for these modules. Specifically, the CBM2
281 from *P. furiosus* used in the current work was able to bind both cellulose and chitin
282 (Estevinho et al., 2018; Talens-Perales, Marín-Navarro, Garrido, Almansa, & Polaina,
283 2017) but its affinity for hemicelluloses has not been previously studied. The fact that
284 the binding yield was higher for F3 (pure cellulose) than for F2 (containing both
285 cellulose and hemicellulose) suggests that the CBM2 used here (from *Pyrococcus*
286 *furiosus*) is more specific for cellulose than it is for hemicellulose. This behaviour may
287 rely on the different chemical structure of cellulose and hemicellulose. While cellulose
288 is composed solely by glucose units interconnected in a linear polysaccharide, which is
289 able to form highly structured fibres, hemicelluloses display a higher diversity of

290 chemical compositions and structures (including linear or branched) (Chen, 2014).
291 Indeed, pure cellulose fraction (F3) showed a more fibrous structure than F2, probably
292 because of the higher heterogeneity of the latter (Figure 4). Binding to the CBM2
293 module is based on the interaction of the linear polysaccharide with three structurally
294 aligned tryptophan residues (Nakamura et al., 2008). Thus, the branching sites in
295 hemicelluloses may interfere with the interaction at this planar binding platform (Figure
296 S1 in Supplementary Material).

297 Another conclusion from the results presented in Figure 3 is that the cellulosic fraction
298 extracted from *P. oceanica* is a better substrate for the immobilization of the hybrid
299 enzyme than that from *A. donax*. Substrate specificity of the CBMs not only relies on
300 the chemical composition but also in the high-order structure of the polysaccharide.
301 Thus, some CBMs are specific for amorphous cellulose while others bind preferentially
302 to crystalline cellulose (Boraston et al., 2004). The polysaccharides extracted from *P.*
303 *oceanica* and *A. donax* may show distinct molecular structural arrangements, not
304 detected by SEM analysis, that explain the differences in TmLac-CBM2 binding yields.

305

306 **3.3. Comparative analysis of the lactase activity of free and immobilized enzyme** 307 **with different cellulosic supports.**

308 After characterizing the suitability of each cellulosic fraction as a support for the
309 enzyme, the activity of enzyme loaded cryogels from both *P. oceanica* and *A. donax*
310 was compared to that of the enzyme in the free form. Furthermore, the activity of the
311 enzyme immobilized in a cellulose film, here named Enzy-film, was also assayed. Since
312 TmLac-CBM2 was not attached to a cellulose film when it was added exogenously
313 (Figure 1), Enzy-film was obtained by enzyme immobilization on the hydrated cellulose

314 from *P. oceanica* and subsequent generation of the film. Such preparation would be
315 more easily handled than the cryogel form.

316 Initial lactase activities (after incubation for 30 minutes) were roughly the same for the
317 enzyme immobilized in the cellulose cryogel from *P. oceanica* or *A. donax* and the free
318 form (around 40 IU/mg enzyme). Taking in account the different immobilization yields
319 of both materials, this represents an activity of 210 and 300 IU/g of support for *A. donax*
320 and *P. oceanica* cellulose, respectively. The immobilization efficiency (defined as the
321 fraction of observed activity after immobilization from the total immobilized activity)
322 (Sheldon & van Pelt, 2013) is 100 % in both cases. However, the Enzy-film was
323 inactive under the assayed conditions (Table S1 in Supplementary material). This may
324 be explained because the dense network of interactions among cellulose fibres in the
325 film may difficult the accessibility of lactose to the enzyme within this matrix. The
326 result obtained with the cellulose cryogel from *P. oceanica* and *A. donax* was better than
327 that reported for bacterial cellulose, which showed immobilization efficiencies of 27 %
328 (freeze-dried) and 52 % (hydrated) for the same enzyme (Estevinho et al., 2018). The
329 high crystallinity of bacterial cellulose (Benito-González et al., 2018; Martínez-Sanz,
330 Lopez-Rubio, & Lagaron, 2011), may provide a compact structure where substrate
331 diffusion is a limiting factor for optimal activity.

332 The hydrolysis of lactose with free and immobilized enzyme was followed for a longer
333 period of incubation, up to 8 hours, using 30 mg of the enzymatically active cryogels
334 and the corresponding amount of enzyme in the free form (Figure 5). Again, no
335 differences were found between free and bound enzymes neither for *P. oceanica* nor for
336 *A. donax* cellulose. Lactose hydrolysis was more efficient with the catalytic cryogel
337 from *P. oceanica*, as a result of the higher immobilization capacity of this support
338 (Figure 3).

339

340 **4. Conclusions**

341 This work shows that the efficiency of bioadsorption of hybrid enzymes mediated by
342 the CBM2 module relies on both the chemical nature and the supra-molecular structure
343 of the polysaccharides used as the support. On the other hand, to assure an efficient
344 action of the bound enzyme, substrate diffusion into the immobilization matrix should
345 not be hampered by a dense network of interactions connecting the polysaccharide
346 fibres. The cellulose extracted from *P. oceanica* and *A. donax* fulfils the requisites for
347 efficient enzyme immobilization and operation. Thus, this approach represents an
348 economic and environmentally-friendly revalorization of a waste material as enzyme
349 support.

350

351 **Acknowledgements**

352 This research was supported by grants from Spain's 'Secretaría de Estado de
353 Investigación, Desarrollo e Innovación' (AGL2016-75245-R), Agencia Estatal de
354 Investigación (AEI, Grant PCI2018-092886) and cofunded by the European Union's
355 Horizon 2020 research and innovation programme (ERA-Net SUSFOOD2). MJF was
356 supported by a Ramon y Cajal contract (RYC2014-158) from the Spanish Ministerio de
357 Economía; Industria y Competitividad. The authors thank the Central Support Service
358 for Experimental Research (SCSIE) of the University of Valencia for the electronic
359 microscopy service.

360

361

362 **References**

363 Adam, A. C., Rubio-Teixeira, J., & Polaina, J. (2004). Lactose: the milk sugar from a

364 biotechnological perspective. *Crit. Rev. Food Sci. Nutr.*, *44*, 553–557.
365 <https://doi.org/https://doi.org/10.1080/10408690490931411>

366 Altschul, S. F., Madden, T. L., Schäffer, A. A., Zhang, J., Zhang, Z., Miller, W., &
367 Lipman, D. J. (1997). Gapped BLAST and PSI-BLAST: A new generation of
368 protein database search programs. *Nucleic Acids Research*.
369 <https://doi.org/10.1093/nar/25.17.3389>

370 Andler, S. M., & Goddard, J. M. (2018). Transforming food waste: how immobilized
371 enzymes can valorize waste streams into revenue streams. *Npj Science of Food*, *2*.
372 <https://doi.org/10.1038/s41538-018-0028-2>

373 Benito-González, I., López-Rubio, A., & Martínez-Sanz, M. (2018). Potential of
374 lignocellulosic fractions from *Posidonia oceanica* to improve barrier and
375 mechanical properties of bio-based packaging materials. *International Journal of*
376 *Biological Macromolecules*, *118*, 542–551.
377 <https://doi.org/10.1016/j.ijbiomac.2018.06.052>

378 Bilal, M., & Iqbal, H. M. N. (2019). Naturally-derived biopolymers: Potential platforms
379 for enzyme immobilization. *International Journal of Biological Macromolecules*,
380 *130*, 462–482. <https://doi.org/10.1016/j.ijbiomac.2019.02.152>

381 Bolivar, J., & Nidetzky, B. (2019). The microenvironment in immobilized enzymes :
382 methods of characterization and its role in determining enzyme performance.
383 *Molecules*, *24*, 8–10. <https://doi.org/https://doi.org/10.3390/molecules24193460>

384 Boraston, A. B., Bolam, D. N., Gilbert, H. J., & Davies, G. J. (2004). Carbohydrate-
385 binding modules: Fine-tuning polysaccharide recognition. *Biochemical Journal*,
386 *382*, 769–781. <https://doi.org/10.1042/BJ20040892>

387 Chen, H. (2014). Chemical composition and structure of natural lignocellulose. In H.
388 Chen (Ed.), *Biotechnology of lignocellulose. Theory and practice* (pp. 25–71).

389 Dordrecht: Springer.

390 Datta, S., Christena, L. R., & Rajaram, Y. R. S. (2013). Enzyme immobilization: an
391 overview on techniques and support materials. *3 Biotech*, *3*, 1–9.
392 <https://doi.org/10.1007/s13205-012-0071-7>

393 Estevinho, B. N., Samaniego, N., Talens-Perales, D., Fabra, M. J., López-Rubio, A.,
394 Polaina, J., & Marín-Navarro, J. (2018). Development of enzymatically-active
395 bacterial cellulose membranes through stable immobilization of an engineered β -
396 galactosidase. *International Journal of Biological Macromolecules*, *115*, 476–482.
397 <https://doi.org/10.1016/j.ijbiomac.2018.04.081>

398 Gänzle, M. G. (2012). Enzymatic synthesis of galacto-oligosaccharides and other
399 lactose derivatives (hetero-oligosaccharides) from lactose. *International Dairy*
400 *Journal*, *22*, 116–122. <https://doi.org/10.1016/j.idairyj.2011.06.010>

401 Harrington, L. K., & Mayberry, J. F. (2008). A re-appraisal of lactose intolerance.
402 *International Journal of Clinical Practice*, *62*, 1541–1546.
403 <https://doi.org/10.1111/j.1742-1241.2008.01834.x>

404 Husain, Q. (2010). Beta galactosidases and their potential applications: a review. *Crit*
405 *Rev Biotechnology*, *30*, 41–62.

406 Itan, Y., Jones, B. L., Ingram, C. J., Swallow, D. M., & Thomas, M. G. (2010). A
407 worldwide correlation of lactase persistence phenotype and genotypes. *BMC*
408 *Evolutionary Biology*, *10*, 36. <https://doi.org/10.1186/1471-2148-10-36>

409 Jesionowski, T., Zdarta, J., & Krajewska, B. (2014). Enzyme immobilization by
410 adsorption: A review. *Adsorption*, *20*, 801–821. [https://doi.org/10.1007/s10450-](https://doi.org/10.1007/s10450-014-9623-y)
411 [014-9623-y](https://doi.org/10.1007/s10450-014-9623-y)

412 Khan, A., Wen, Y., Huq, T., & Ni, Y. (2018). Cellulosic nanomaterials in food and
413 nutraceutical applications: a review. *Journal of Agricultural and Food Chemistry*,

414 66, 8–19. <https://doi.org/10.1021/acs.jafc.7b04204>

415 Khiari, R., & Belgacem, M. N. (2017). Potential for using multiscale *Posidonia*
416 *oceanica* waste: Current status and prospects in material science. In M. Jawaid, P.
417 Tahir, & N. Saba (Eds.), *Lignocellulosic fibre and biomass-based composite*
418 *materials: processing, properties and applications* (pp. 447–471). Elsevier Ltd.
419 <https://doi.org/10.1016/B978-0-08-100959-8.00021-4>

420 Lambert, A. M., Dudley, T. L., & Saltonstall, K. (2010). Ecology and impacts of the
421 large-statured invasive grasses *Arundo donax* and *Phragmites australis* in North
422 America. *Invasive Plant Science and Management*, 3, 489–494.
423 <https://doi.org/10.1614/ipsm-d-10-00031.1>

424 Lombard, V., Golaconda Ramulu, H., Drula, E., Coutinho, P. M., & Henrissat, B.
425 (2014). The carbohydrate-active enzymes database (CAZy) in 2013. *Nucleic Acids*
426 *Research*, 42, 490–495. <https://doi.org/10.1093/nar/gkt1178>

427 Lu, P., & Hsieh, Y. Lo. (2012a). Cellulose isolation and core-shell nanostructures of
428 cellulose nanocrystals from chardonnay grape skins. *Carbohydrate Polymers*, 87,
429 2546–2553. <https://doi.org/10.1016/j.carbpol.2011.11.023>

430 Lu, P., & Hsieh, Y. Lo. (2012b). Preparation and characterization of cellulose
431 nanocrystals from rice straw. *Carbohydrate Polymers*, 87, 564–573.
432 <https://doi.org/10.1016/j.carbpol.2011.08.022>

433 Marín-Navarro, J., Talens-Perales, D., Oude-Vrielink, A., Cañada, F. J., & Polaina, J.
434 (2014). Immobilization of thermostable β -galactosidase on epoxy support and its
435 use for lactose hydrolysis and galactooligosaccharides biosynthesis. *World Journal*
436 *of Microbiology and Biotechnology*, 30, 989–998. [https://doi.org/10.1007/s11274-](https://doi.org/10.1007/s11274-013-1517-8)
437 013-1517-8

438 Martínez-Sanz, M., Lopez-Rubio, A., & Lagaron, J. M. (2011). Optimization of the

439 nanofabrication by acid hydrolysis of bacterial cellulose nanowhiskers.
440 *Carbohydrate Polymers*, 85, 228–236.
441 <https://doi.org/10.1016/j.carbpol.2011.02.021>

442 Mislovičová, D., Masárová, J., Vikartovská, A., Gemeiner, P., & Michalková, E.
443 (2004). Biospecific immobilization of mannan-penicillin G acylase
444 neoglycoenzyme on Concanavalin A-bead cellulose. *Journal of Biotechnology*,
445 110, 11–19. <https://doi.org/10.1016/j.jbiotec.2004.01.006>

446 Nakamura, T., Mine, S., Hagihara, Y., Ishikawa, K., Ikegami, T., & Uegaki, K. (2008).
447 Tertiary structure and carbohydrate recognition by the chitin-binding domain of a
448 hyperthermophilic chitinase from *Pyrococcus furiosus*. *Journal of Molecular*
449 *Biology*, 381, 670–680. <https://doi.org/10.1016/j.jmb.2008.06.006>

450 Nguyen, H. H., Lee, S. H., Lee, U. J., Fermin, C. D., & Kim, M. (2019). Immobilized
451 enzymes in biosensor applications. *Materials*, 12, 1–34.
452 <https://doi.org/10.3390/ma12010121>

453 Oliveira, C., Guimarães, P. M. R., & Domingues, L. (2011). Recombinant microbial
454 systems for improved β -galactosidase production and biotechnological
455 applications. *Biotechnology Advances*, 29, 600–609.
456 <https://doi.org/10.1016/j.biotechadv.2011.03.008>

457 Pilavtepe, M., Celiktas, M. S., Sargin, S., & Yesil-Celiktas, O. (2013). Transformation
458 of *Posidonia oceanica* residues to bioethanol. *Industrial Crops and Products*, 51,
459 348–354. <https://doi.org/10.1016/j.indcrop.2013.09.020>

460 Rao, P., & Rathod, V. (2018). Valorization of food and agricultural waste: a step
461 towards greener future. *Chemical Record*, 19, 1858–1871.
462 <https://doi.org/10.1002/tcr.201800094>

463 Ricardi, N. C., de Menezes, E. W., Valmir Benvenuto, E., da Natividade Schöffner, J.,

464 Hackenhaar, C. R., Hertz, P. F., & Costa, T. M. H. (2018). Highly stable novel
465 silica/chitosan support for β -galactosidase immobilization for application in dairy
466 technology. *Food Chemistry*, 246, 343–350.
467 <https://doi.org/10.1016/j.foodchem.2017.11.026>

468 Sen, P., Nath, A., Bhattacharjee, C., Chowdhury, R., & Bhattacharya, P. (2014). Process
469 engineering studies of free and micro-encapsulated β -galactosidase in batch and
470 packed bed bioreactors for production of galactooligosaccharides. *Biochemical*
471 *Engineering Journal*, 90, 59–72. <https://doi.org/10.1016/j.bej.2014.05.006>

472 Sharma, S. K., & Leblanc, R. M. (2017). Biosensors based on β -galactosidase enzyme:
473 Recent advances and perspectives. *Analytical Biochemistry*, 535, 1–11.
474 <https://doi.org/10.1016/j.ab.2017.07.019>

475 Sheldon, R. A., & van Pelt, S. (2013). Enzyme immobilisation in biocatalysis: Why,
476 what and how. *Chemical Society Reviews*, 42, 6223–6235.
477 <https://doi.org/10.1039/c3cs60075k>

478 Sirisha, V., Jain, A., & Jain, A. (2016). Enzyme immobilization: An overview on
479 methods, support material, and applications of immobilized enzymes. *Adv Food*
480 *Nutr Res*, 79, 179–211.

481 Talens-Perales, D., Marín-Navarro, J., Garrido, D., Almansa, E., & Polaina, J. (2017).
482 Fixation of bioactive compounds to the cuticle of *Artemia*. *Aquaculture*, 474, 95–
483 100. <https://doi.org/10.1016/j.aquaculture.2017.03.044>

484 Urrutia, P., Bernal, C., Wilson, L., & Illanes, A. (2018). Use of chitosan
485 heterofunctionality for enzyme immobilization: β -galactosidase immobilization for
486 galacto-oligosaccharide synthesis. *International Journal of Biological*
487 *Macromolecules*, 116, 182–193. <https://doi.org/10.1016/j.ijbiomac.2018.04.112>

488 Wolf, M., Gasparin, B. C., & Paulino, A. T. (2018). Hydrolysis of lactose using β -D-

489 galactosidase immobilized in a modified Arabic gum-based hydrogel for the
490 production of lactose-free/low-lactose milk. *International Journal of Biological*
491 *Macromolecules*, *115*, 157–164. <https://doi.org/10.1016/j.ijbiomac.2018.04.058>
492 Yushkova, E., Nazarova, E., Matyuhina, A., Noskova, A., Shavronskaya, D.,
493 Vinogradov, V., ... Krivoshapkina, E. (2019). Application of immobilized
494 enzymes in the food industry. *Journal of Agricultural and Food Chemistry*, *67*,
495 11553–11567. <https://doi.org/https://doi.org/10.1021/acs.jafc.9b04385>
496

497 **Figure legends.**

498

499 **Figure 1.** Immobilization yield of TmLac-CBM2 to cellulose (F3) from *P. oceanica* in
500 different physical states. Error bars represent standard deviation of triplicates.
501 Homogeneous groups are indicated with lower case letters (significance level $\alpha=0,05$);
502 nd: not detected.

503

504 **Figure 2.** SEM images of a film (A) and cryogel (B) obtained from cellulose (F3) from
505 *P. oceanica*

506

507 **Figure 3.** Immobilization yield of TmLac-CBM2 to cellulose fractions (F2 and F3)
508 from *P. oceanica* and *A. donax* in the form of cryogel. Error bars represent standard
509 deviation of triplicates. Homogeneous groups are indicated with lower case letters
510 (significance level $\alpha=0,05$).

511

512 **Figure 4.** SEM images of cryogels obtained from fractions 2 (F2P and F2C) and 3 (F3P
513 and F3C) isolated from *P. oceanica* (F2P and F3P) or *A. donax* (F2C and F3C).

514

515 **Figure 5.** Kinetics of lactose hydrolysis with bioactivated cryogels from *P. oceanica*
516 (PO) or *A. donax* (AD) or with the equivalent amounts of enzyme in the free form (CP
517 and CO, respectively). Error bars represent standard deviation of triplicates.

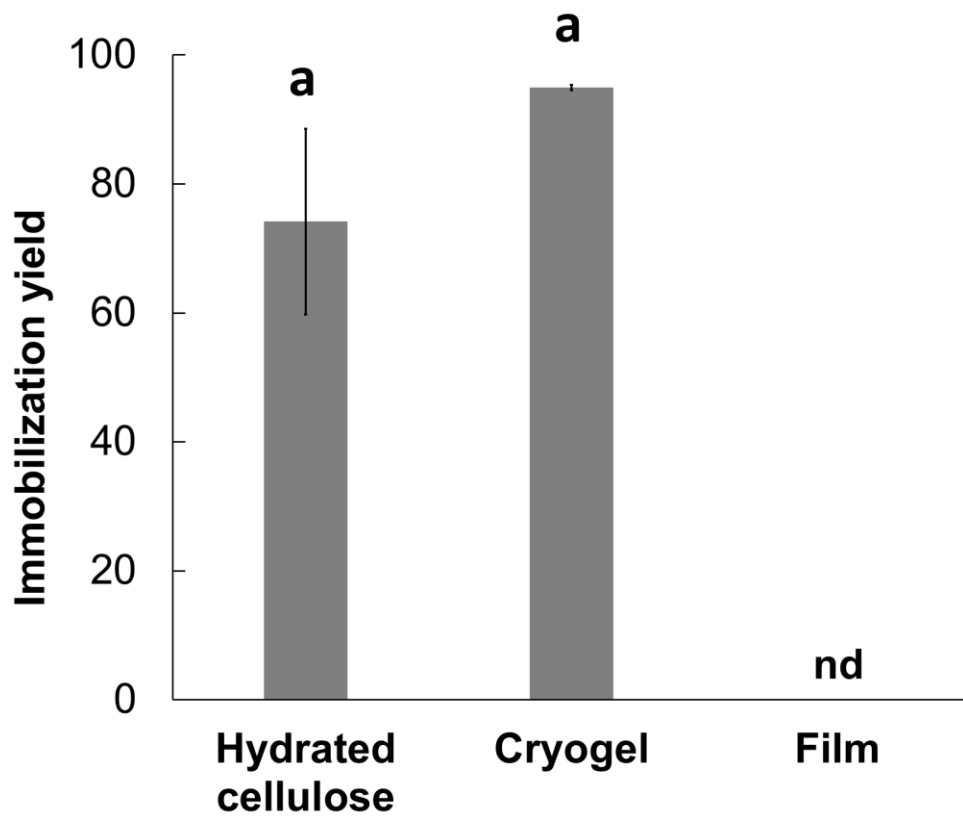
518

519

520

521

522 **Figure 1**



523

524

525

526

527

528

529

530

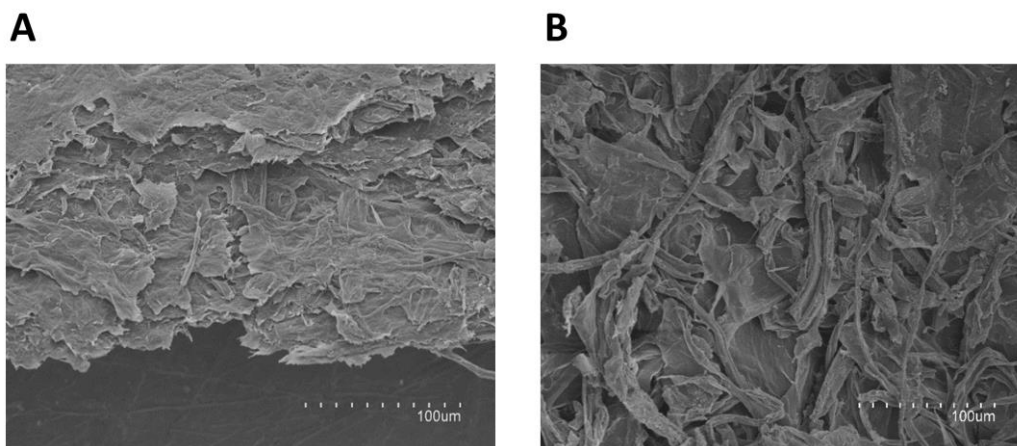
531

532

533

534

535 **Figure 2**



536

537

538

539

540

541

542

543

544

545

546

547

548

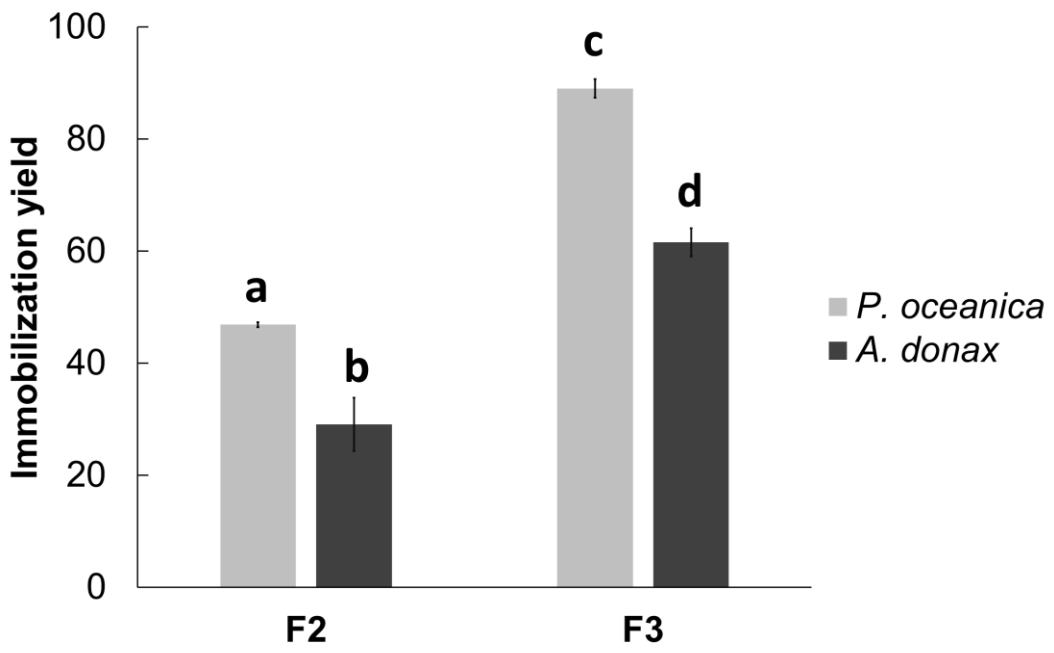
549

550

551

552

553 **Figure3**



554

555

556

557

558

559

560

561

562

563

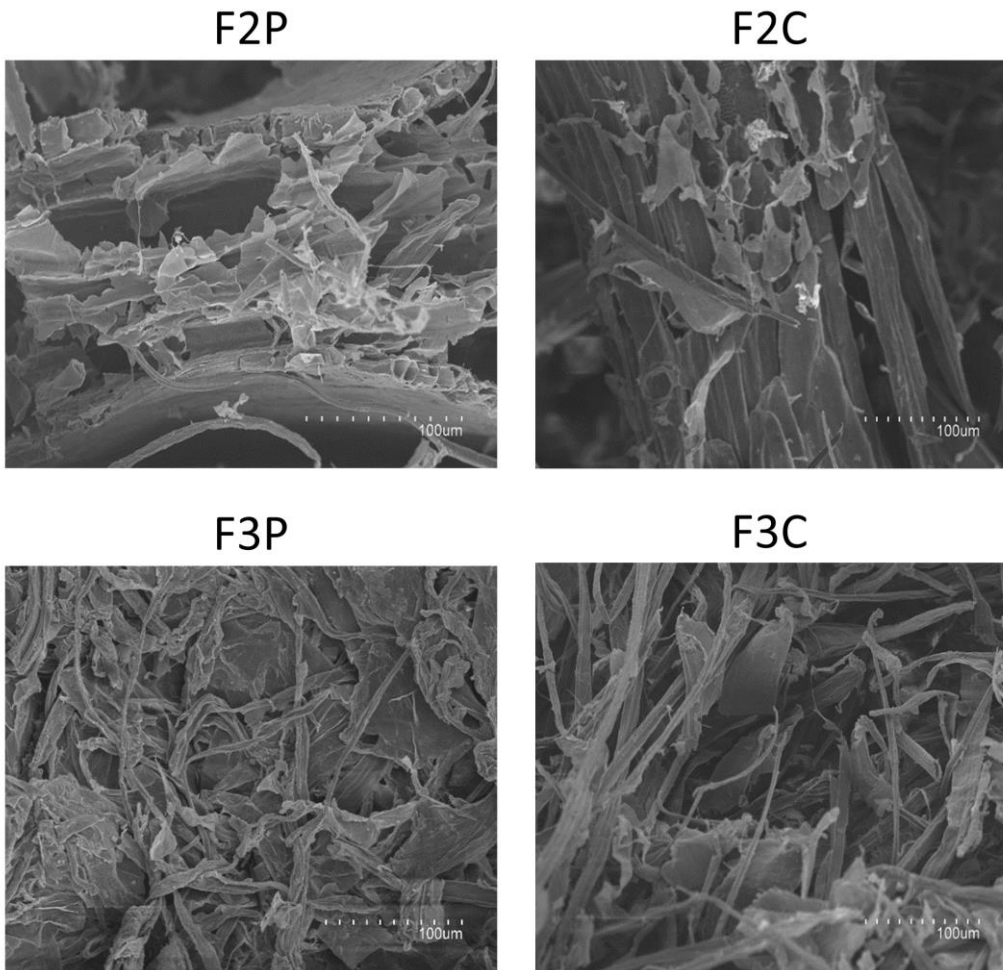
564

565

566

567

568



570

571

572

573

574

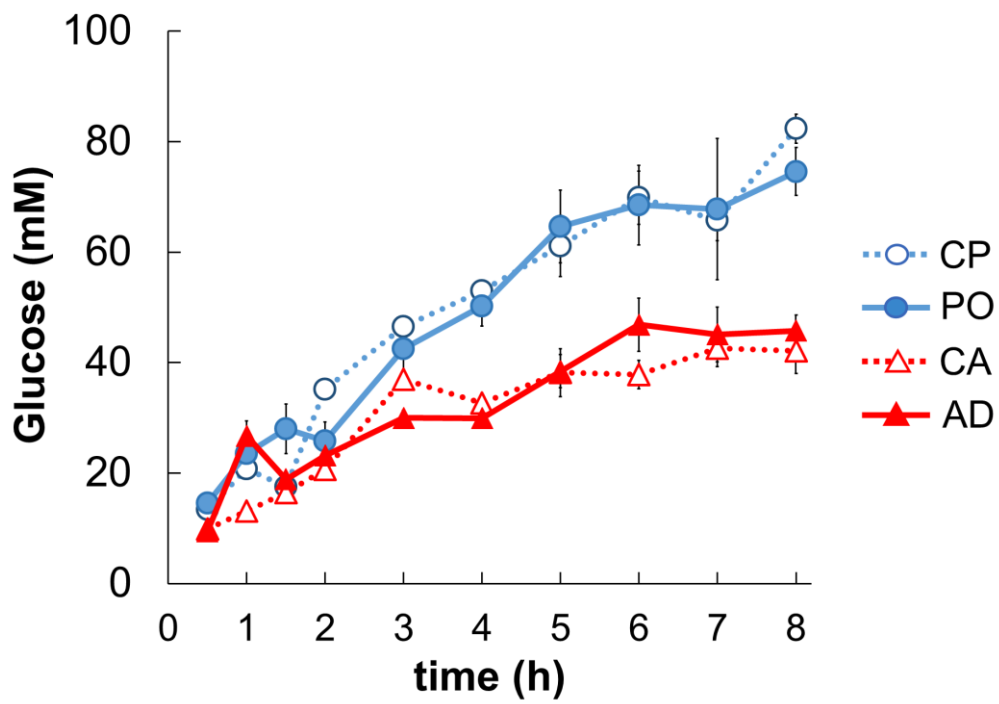
575

576

577

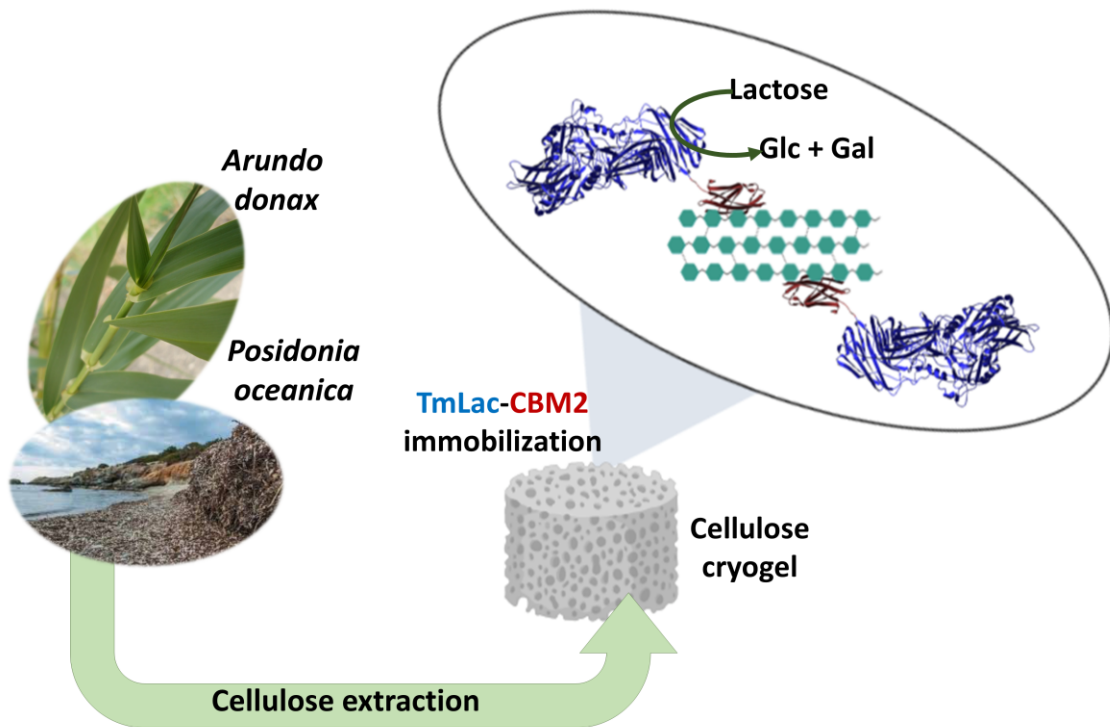
578

579 **Figure 5**



580

581 **Graphical Abstract**



582